

03  
**Features of propagation and absorption of electromagnetic signals in periodic structures of conducting and dielectric layers**

© A.V. Bogatskaya<sup>1,2,3</sup>, N.V. Klenov<sup>1</sup>, P.M. Nikiforova<sup>1,4</sup>, A.M. Popov<sup>1,2</sup>, A.E. Schegolev<sup>3,4</sup>

<sup>1</sup> Department of Physics, Moscow State University, Moscow, Russia

<sup>2</sup> Lebedev Physical Institute, Russian Academy of Sciences, Moscow, Russia

<sup>3</sup> Moscow Technical University of Communications and Informatics, Moscow, Russia

<sup>4</sup> Skobeltsyn Institute of Nuclear Physics, Moscow State University, Moscow, Russia

e-mail: annabogatskaya@gmail.com

Received on December 20, 2021

Revised on December 20, 2021

Accepted on December 30, 2021

Different regimes of electromagnetic signal transmission through heterostructures formed by a sequence of conducting and non-conducting layers are discussed for various ratios between the frequency of radiation and the transport frequency of electron scattering in the conducting layers. Possibility to increase the efficiency of detecting or filtering electromagnetic radiation in a wide range of frequency range (from subTHz to far IR) in such structures is analyzed.

**Keywords:** propagation of electromagnetic waves in heterostructures, resonant tunneling, THz-IR detectors, bolometers.

DOI: 10.21883/EOS.2022.04.53722.48-21

## Introduction

Existing THz-IR detectors can be divided into two groups according to the principle of operation: photonic and thermal ones [1–8]. In photon detectors, radiation is absorbed inside the material by means of internal photoelectric effect, i.e. direct interaction of photons with charge carriers. Such detectors, in contrast to thermal ones, have selective frequency sensitivity; they are characterized by high-speed performance and high signal-to-noise ratio. However, terahertz (THz) radiation is characterized by low photon energy; therefore, photonic THz devices with quantum transitions can operate only at low temperatures, which is extremely inconvenient for practical use. The principle of operation of thermal detectors is based on the conversion of incident radiation into heat, followed by the conversion of the heat flux into an electrical signal. Thermal detectors include various microbolometers (metal-, semiconductor ones). The advantages of such detectors are the simplicity of design and the absence of the need for cryogenic cooling, which significantly reduces the energy consumption during operation and the cost of the devices. The disadvantage of THz bolometric detectors is their low sensitivity. In works [9–11], the possibility of increasing the sensitivity of bolometric receivers for the cases of quasi-monochromatic and broad-band THz radiation was studied. As noted in [9], the bolometer efficiency can be significantly increased if the dielectric layer, behind the absorbing sensitive element is placed, which plays the role of an electromagnetic resonator and ensures the resonant electromagnetic transmission through conducting layer with supercritical electron concentration [12, 13]. It

was shown that such a resonant transition is accompanied by effective absorption of the energy of an electromagnetic wave in the conductive layer at the same frequency. The possibility of increasing the spectral width of detection by replacing one dielectric layer with a heterostructure of a periodic sequence of conductive- and dielectric layers was considered in [10,11] It was shown in [10,11], that in such a heterostructure, similarly to the allowed bands of photonic crystal, bands will be formed, within which an increase in absorption is also possible. But, in contrast to photonic crystal, the transmission- and absorption bands are formed differently in the heterostructure under study.

In this work, the features associated with different modes of transmission of electromagnetic signals through a heterostructure depending on the ratio between the frequency of detected radiation and the transport frequency of scattering of charge carriers in conducting layers are considered, and the possibility of creating both detectors and filters of electromagnetic radiation in a wide frequency range (from subterahertz to far IR) based on such structures are discussed. The characteristic form of the structures studied below in the case of different numbers of conductive- and non-conductive layers is shown in Fig. 1.

## Problem formulation. Simulation of electromagnetic wave propagation in periodic heterostructure

The spatial structure of the electric field of a monochromatic wave with frequency  $\omega$  incident normally on a spatially-nonhomogeneous medium with permittivity  $\varepsilon_\omega(z)$

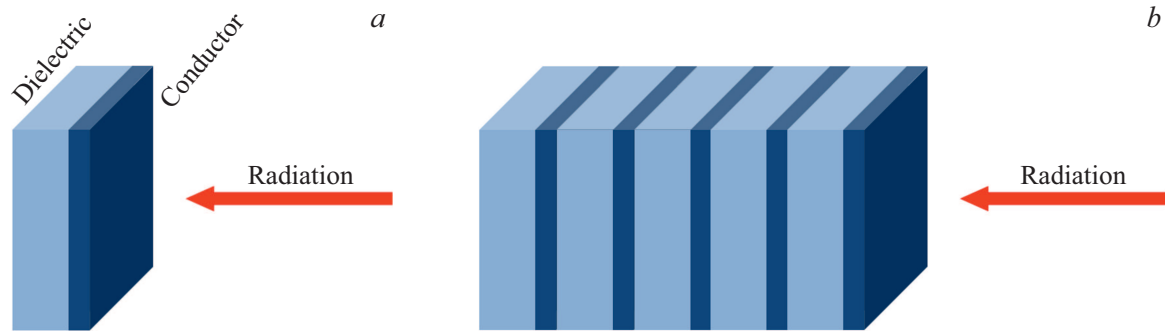


**Figure 1.** Heterostructure of the sequence of  $N$  conductive and non-conductive layers based on doped and undoped gallium arsenide: (a)  $N = 1$ , (b)  $N = 5$ .

( $z$  directed normal to the surface) is described by the Helmholtz equation for electric field strength  $E(z)$ :

$$\frac{d^2 E(z)}{dz^2} + \frac{\omega^2}{c^2} \varepsilon_\omega(z) E(z) = 0, \quad (1)$$

where, according to [9–11], the permittivity can be submitted in a form

$$\varepsilon_\omega = \begin{cases} \varepsilon_0, & 0 < z \leq a, \\ & \text{in dielectric layer,} \\ \varepsilon_0 - \frac{\omega_p^2}{\omega^2 + \nu^2} + i \frac{\omega_p^2 \nu}{(\omega^2 + \nu^2)\omega}, & a \leq z \leq a + b, \\ & \text{in conductive layer,} \\ \varepsilon_{\text{air}}, & z \geq a + b, \\ & \text{outside the periodic structure.} \end{cases} \quad (2)$$

Here  $a$  and  $b$  are thicknesses of the dielectric and conducting layers, respectively,  $\varepsilon_0$  is dielectric permittivity of the undoped layer. In conductive layers for the permittivity, we used the expression from the Drude theory,  $\omega_p^2 = 4\pi e^2 n_e / m^*$  is plasma frequency, determined by the quantity  $n_e$  ( $n_e$  is concentration of  $n$ -type carriers),  $m^*$  is effective mass of  $n$ -type carriers,  $\nu$  is effective (transport) collision frequency,  $\varepsilon_{\text{air}} \approx 1$  is permittivity of air. In this case, it is further assumed that an perfect reflecting surface in the plane  $z = 0$  is located. It is known that typical transport frequencies  $\nu$  of the most commonly used semiconductors (GaAs, Ge, Si) range from  $8 \cdot 10^{11}$  to  $3 \cdot 10^{12} \text{ s}^{-1}$ , therefore, in the case of IR radiation, the inequality  $\nu \ll \omega \ll \omega_p$  is satisfied, while in the case of subterahertz radiation, the reverse case  $\omega < \nu \ll \omega_p$ . As will be shown below, the problem has significantly different solutions depending on the ratio between the transport frequency  $\nu$  and the frequency of the propagating radiation  $\omega$  (in this case, we assume that  $\omega, \nu \ll \omega_p$ ).

For the IR frequency range, in the zeroth approximation in the small parameter  $\nu/\omega_p$ , the permittivity of the conducting layer can be written as  $\varepsilon_\omega \approx \varepsilon_0 - \frac{\omega_p^2}{\omega^2}$ . Then

equation (1) can be rewritten in the form

$$\frac{d^2 E(z)}{dz^2} + \frac{\omega^2}{c^2} \left( \varepsilon_0 - \frac{\omega_p^2}{\omega^2} \right) E(z) = 0. \quad (3)$$

It's plain to see that this equation is mathematically analogous to the stationary Schrödinger equation for a particle of mass  $m$  in potential  $V(z)$ :

$$-\frac{\hbar^2}{2m} \frac{d^2 \psi(z)}{dz^2} + V(z) \psi(z) = \xi \psi(z), \quad (4)$$

where  $\psi(z)$  is the wave function of the stationary state with energy  $\xi$ . Thus, from the point of view of quantum mechanics, the presence of a dielectric layer (resonator) located behind the conducting plasma coating is analogous to the presence of a potential well located behind the potential barrier. Then the solution of equation (3), which describes the penetration of an electromagnetic field through the region with supercritical electron concentration, can be interpreted in terms of analogy with quantum mechanics as tunneling of particles through potential barrier. In this case, if the frequency of the incident field coincides with the frequency of the eigenmodes of the resonator, the effect of resonant tunneling of the field through „the plasma barrier“ will be observed, which will lead to effective filling of the dielectric resonator with an electromagnetic field.

To calculate the absorption of field energy in the structure, it is necessary to take into account the presence of the imaginary part of the permittivity:

$$\varepsilon_\omega \approx \varepsilon_0 - \frac{\omega_p^2}{\omega^2} + i \frac{\omega_p^2 \nu}{\omega^3}. \quad (5)$$

Below, layers of doped GaAs are considered as conductors, and layers of undoped GaAs are considered as dielectrics. In this case, the doping level is chosen so that the frequency of the incident field is below the critical one, and the penetration depth  $\delta$  is of the order of the thickness of the conductive layer. For the case  $\nu \ll \omega \ll \omega_p$  under consideration, the penetration depth can be estimated from the formula  $\delta \approx c/\omega_p$ , which imposes a limitation on the thickness of the doped semiconductor.

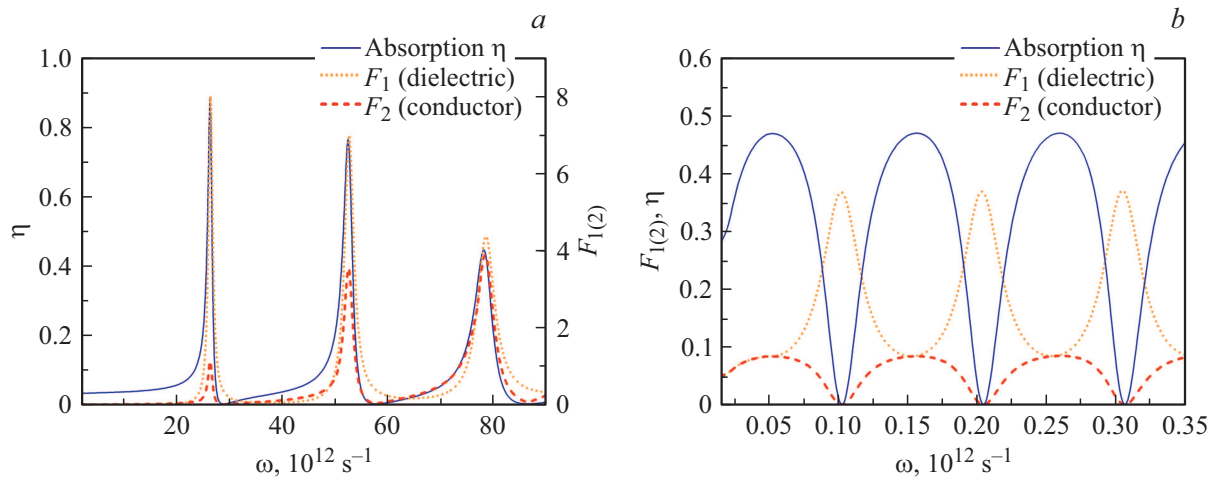


**Figure 2.** Absorption  $\eta$  and filling factors  $F_{1,2}$  depending on the frequency of the incident radiation. Structure parameters: (a) dielectric layer thickness  $a = 9.5 \mu\text{m}$ , conductive layer thickness  $b = 1 \mu\text{m}$ , plasma frequency  $\omega_p = 3 \cdot 10^{14} \text{s}^{-1}$ , transport frequency in GaAs  $\nu = 3.09 \cdot 10^{12} \text{s}^{-1}$ ; (b)  $a = 2800 \mu\text{m}$ ,  $b = 1 \mu\text{m}$ ,  $\omega_p = 7.6 \cdot 10^{13} \text{s}^{-1}$ ,  $\nu = 3.09 \cdot 10^{12} \text{s}^{-1}$ .

It is convenient to characterize the efficiency of electric field penetration inside the dielectric resonator and „plasma barrier“ by the filling factor [13] defined as

$$F_{1,2}(\omega) = \max \left\{ \frac{|E_{1(2)}|^2}{|E_0|^2} \right\}, \quad (6)$$

where  $E_{1(2)}$  — are the maximum values of the electric field strength of the wave that has passed into the region of the dielectric (conductive) layer of the wave, obtained from the numerical solution of the Helmholtz equation (1), and  $E_0$  — strength of the electric field of the incident wave.

Another situation arises in low-frequency fields, when  $\omega \ll \nu \ll \omega_p$ . In this case, the imaginary part of the permittivity in the conducting layer becomes the main term, and in the low-frequency approximation,  $\epsilon_\omega \approx i \frac{\omega_p^2}{\nu \omega}$  can be written. The Helmholtz equation in the conducting layer takes the form

$$\frac{d^2 E(z)}{dz^2} + i \frac{\omega \omega_p^2}{\nu c^2} E(z) = 0. \quad (7)$$

It is obvious that in its structure this equation differs greatly from equation (3) for the case of a high-frequency field. Therefore, it is natural to expect a different character of electromagnetic wave propagation through the heterostructure.

### Simulation results. Formation of electromagnetic wave transmission and absorption zones in a periodic heterostructure of doped and undoped GaAs

Fig. 2, a shows the filling factors for the dielectric layer  $F_1$  and for the conducting layer  $F_2$  depending on

the radiation frequency, obtained by numerical integration of equations (1), (2) in the case of  $\omega \gg \nu$ . Also, the absorption curve  $\eta$  as a function of frequency is shown Fig. 2, a. Absorption was calculated by us using the following formula [10]:

$$\eta(\omega) = \frac{\omega_p^2 \nu}{\omega^2 + \nu^2} \frac{\int E^2(z) dz}{c E_0^2}. \quad (8)$$

The integral in (8) is taken around the region of the conducting layer.

As can be seen, the effective tunneling of an electromagnetic wave into the resonator at certain frequencies is accompanied by a significant penetration of the field into the conducting layer at the same frequencies, which leads to an increase in the fraction of absorbed energy. In this case, the presence of the squared frequency in the denominator (8) leads to the fact that the maximum absorption is observed at the minimum value of the resonant frequency. The position of resonant frequencies can be determined from the condition:

$$\omega_n \approx \frac{\pi c}{a \sqrt{\epsilon_0}} n, \quad (9)$$

where  $a$  is thickness of the dielectric layer (undoped GaAs),  $n$  is resonance number. Under the conditions under consideration, such structure provides absorption on the order of 80–90% of the incident radiation energy at frequencies determined by expression (9). Later, it was condition (9) that underlay the choice of the thickness of dielectric layers for analyzing the passage of an electromagnetic wave in the  $\nu \ll \omega \ll \omega_p$  and  $\omega \ll \nu \ll \omega_p$ .

Qualitatively different field structure in the system arises in the low-frequency case  $\omega \ll \nu \ll \omega_p$ . If we put the penetration depth, determined in this case by the expression  $\delta \approx \frac{c}{\omega_p} \sqrt{\frac{2\nu}{\omega}}$ , on the order of the thickness of the conducting layer, the penetration of the field into the conductive and

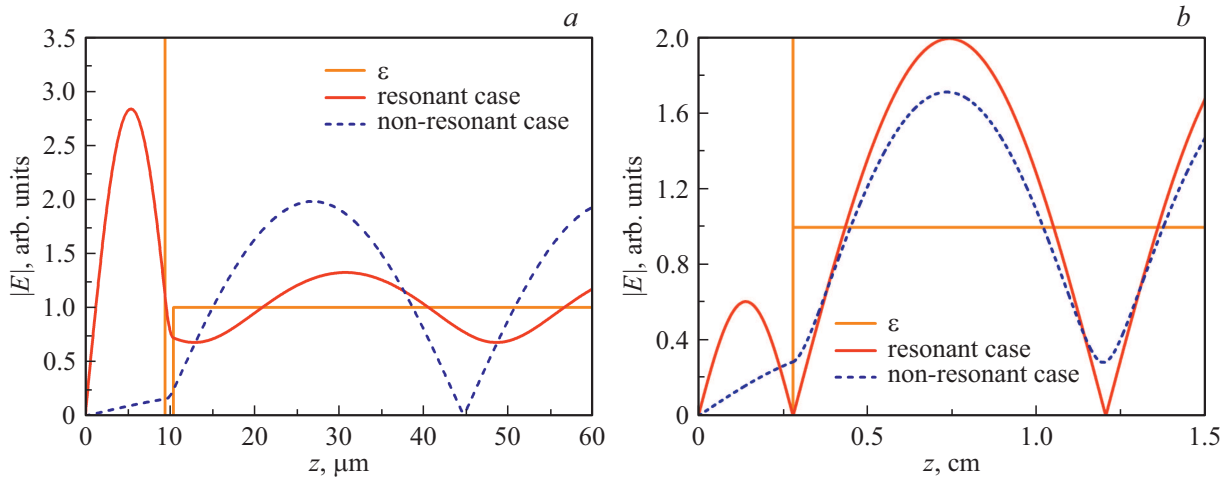


**Figure 3.** Spatial distribution of electric field strength. Structure parameters: (a) dielectric layer thickness  $a = 9.5 \mu\text{m}$ , conductive layer thickness  $b = 1 \mu\text{m}$ , plasma frequency  $\omega_p = 3 \cdot 10^{14} \text{s}^{-1}$ , transport frequency in GaAs  $\nu = 3.09 \cdot 10^{12} \text{s}^{-1}$ ; (b)  $a = 2800 \mu\text{m}$ ,  $b = 1 \mu\text{m}$ ,  $\omega_p = 7.6 \cdot 10^{13} \text{s}^{-1}$ ,  $\nu = 3.09 \cdot 10^{12} \text{s}^{-1}$ .

non-conductive regions of the structure turns out to be insignificant, due to which the signal absorption will also be negligible. Therefore, below we consider the case when the skin depth  $\delta$  is much larger than the thickness of the conducting layer. For such situation, Fig. 2, *b* shows the filling factors for the dielectric layer  $F_1$  and for the conducting layer  $F_2$ , as well as the absorption curve  $\eta$ . It can be seen that in this case, the effective penetration of the electric field into the dielectric resonator is not accompanied by an increase in the field strength inside the conducting layer (Fig. 2, *b*). On the contrary, at frequencies corresponding to the frequencies of the resonator eigenmodes, absorption minima are observed.

To explain the difference between the resonance curves in the low- and high-frequency cases, let us consider the spatial distribution of the modulus of the electric field strength in the structure under study (Fig. 3). In the high-frequency case, when the field frequency coincides with the frequency of one of the resonator modes (the graph is plotted for the field frequency coinciding with the frequency of the first mode), the field penetrates well into the dielectric layer, which is accompanied by effective absorption in the conducting layer. The dashed curve on the graph shows the field distribution in the case when a material with  $\epsilon = 1$  is taken as a dielectric under the conducting layer. The frequencies for both fields presented on the graph are the same, but in the case of the dashed curve, this frequency is resonant already. It can be seen that, in the absence of nonresonance, the penetration of the field into the conducting region is much smaller.

Figure 3, *b* shows the spatial distribution of the modulus of the electric field strength for the  $\omega \ll \nu \ll \omega_p$  case. In the resonant case, the field also effectively fills the resonator. In this case, the field distribution is same that if exactly half the wavelength fits across the dielectric width, a node is formed in the conductive layer, and

since the conductive layer is thin enough (compared to the wavelength), absorption for resonant frequencies is minimal. As before, the dashed line on the graph represents the field distribution in the case when there is a dielectric with  $\epsilon = 1$  under the conducting layer. In this case, the field fills the resonator worse, but penetrates better into the conducting layer. Thus, in the low-frequency case, the introduction of dielectric behind the conductive layer reduces the absorption of field energy for a set of resonant frequencies.

Further, we consider the features of propagation and absorption of electromagnetic waves in heterostructures consisting of a sequence of five conducting and dielectric layers.

Figure 4, *a* shows the filling factors<sup>1</sup> dielectric,  $F_1$ , and conductive,  $F_2$ , layers for IR radiation ( $\nu \ll \omega \ll \omega_p$ ), as well as the share of energy absorption in the totality of conductive layers. It can be seen that in this case, with an increase in the number of layers, a band structure of field modes (photonic crystal) is formed, similar to how allowed energy bands are formed in solid state. In this case, the position of the allowed zones is determined by the width of the dielectric layer and the value of the permittivity (9), and their width — by the connection between adjacent dielectric layers, i.e., the probability „of tunneling“ of the field through the separating dielectric layers „potential barrier“ (conductive layer). The value of this bond can be controlled by changing the width of the doped layers or the degree of doping [10,11]. With an increase in the frequency of the acting radiation, the coupling between the layers increases, which leads to more efficient „tunneling“ of the field into the structure and an increase in absorption.

In the opposite case ( $\omega \ll \nu \ll \omega_p$ ), numerical simulation showed that with an increase in the number of

<sup>1</sup> In this case, the filling factor (6) includes the maximum field value in the set of dielectric (conductive) layers.

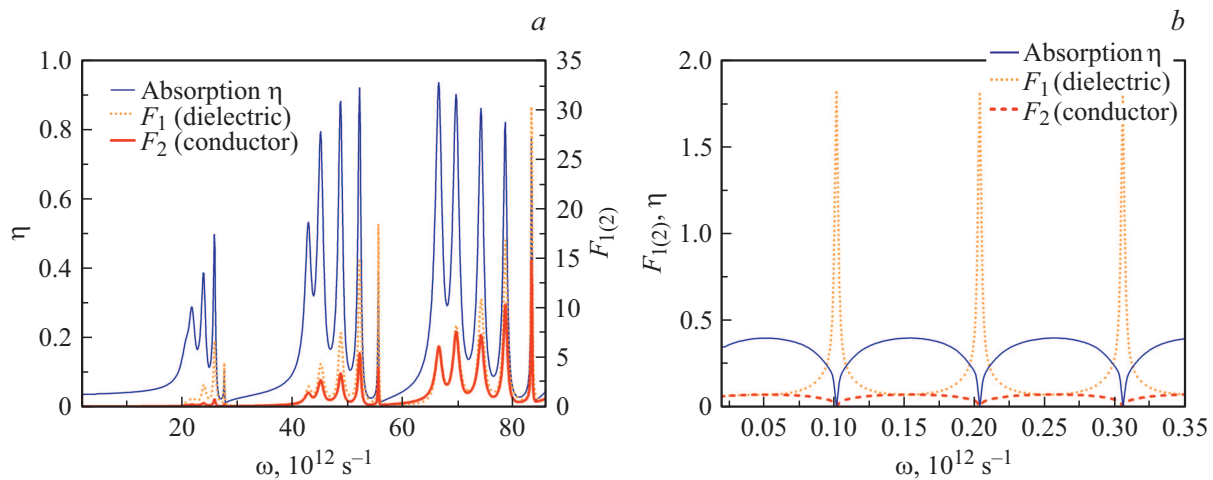


**Figure 4.** Absorption  $\eta$  and filling factors  $F_{1,2}$  depending on the frequency of the incident radiation. Structure parameters: (a) dielectric layer thickness  $a = 9.5 \mu\text{m}$ , conductive layer thickness  $b = 1 \mu\text{m}$ , plasma frequency  $\omega_p = 3 \cdot 10^{14} \text{s}^{-1}$ , transport frequency in GaAs  $\nu = 3.09 \cdot 10^{12} \text{s}^{-1}$ ; (b)  $a = 2800 \mu\text{m}$ ,  $b = 1 \mu\text{m}$ ,  $\omega_p = 7.6 \cdot 10^{13} \text{s}^{-1}$ ,  $\nu = 3.09 \cdot 10^{12} \text{s}^{-1}$ . The case of five conducting layers is considered.

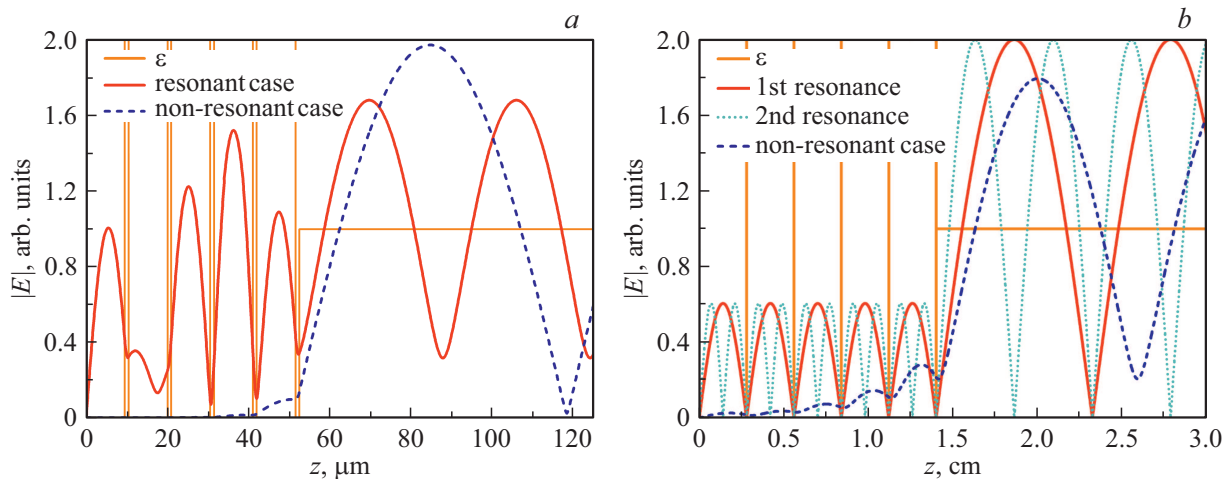


**Figure 5.** Spatial distribution of electric field strength. Structure parameters: (a) dielectric layer thickness  $a = 9.5 \mu\text{m}$ , conductive layer thickness  $b = 1 \mu\text{m}$ , plasma frequency  $\omega_p = 3 \cdot 10^{14} \text{s}^{-1}$ , transport frequency in GaAs  $\nu = 3.09 \cdot 10^{12} \text{s}^{-1}$ ; (b)  $a = 2800 \mu\text{m}$ ,  $b = 1 \mu\text{m}$ ,  $\omega_p = 7.6 \cdot 10^{13} \text{s}^{-1}$ ,  $\nu = 3.09 \cdot 10^{12} \text{s}^{-1}$ .

dielectric layers, no band structure of field modes is formed. Instead, narrow levels appear, corresponding to the passage of the wave at resonant frequencies. Absorption minima are observed at the same frequencies (Fig. 4, b), moreover the spectral width of the levels decreases with an increase in the number of layers.

An illustration of the formation of absorption- and transmission-zones in the low- and high-frequency cases are the spatial distributions of the electric field strength for both cases (Fig. 5, a, b). Comparative analysis of the two graphs shows that both in the high-frequency case (Fig. 5, a) and in the low-frequency case,  $\omega \ll \nu \ll \omega_p$  (Fig. 5, b), at certain frequencies, the field penetrates into the heterostructure and fills the sequence of dielectric resonators. However, in this case, the sequence of dielectric resonators turns out to be significantly different: in the case shown in Fig. 4, a, filling

the dielectric resonators with the field is accompanied by increase in absorption in the conductive layers (see solid curve). On the contrary, in the case shown in Fig. 4, b, for frequencies coinciding with the resonator eigenmodes, the field practically does not penetrate into the conducting layers, and it is at these resonant frequencies that the minima of the dependence of the absorbed energy on radiation frequencies.

## Conclusion

Thus, it is shown that the nature of propagation and absorption of electromagnetic waves in heterostructures based on a sequence of conducting and dielectric layers differs greatly for two regimes determined by the ratio of the

field frequency and the transport frequency of scattering of charge carriers in conducting layers:  $\nu \ll \omega$  (high frequency mode) and  $\nu \gg \omega$  (low frequency mode). It is shown that an increase in the fraction of absorbed energy of an incident wave when its frequency coincides with the frequency of one of the modes of the dielectric resonator (or when it enters the allowed band in the case of a structure consisting of a sequence of several dielectric and conducting layers) occurs only when the frequency of the incident radiation is greater than transport frequency of carrier scattering in conducting layers. For the  $\nu \gg \omega$  case, on the contrary, the absorption minimum at frequencies of electromagnetic waves corresponding to their resonant passage is observed. Increase in the number of layers in such a heterostructure leads to a narrowing of the resonant signal transmission bands. From the point of view of practical applications, the use of such structures for the purpose of increasing the efficiency of bolometric detection is possible in the high-frequency mode. The low frequency mode implies the use of such heterostructures as a radiation filter, which may be relevant for a number of integrated photonics devices [14–16].

## Funding

P.M. Nikiforova expresses her gratitude for the support of the Foundation for Development of Theoretical Physics and Mathematics „BAZIS“ (project 21-2-1-15-1). A.V. Bogatskaya is grateful for the support of the Foundation for Scholarships of the President of the Russian Federation (SP-3120.2022.3). N.V. Klenov is the winner of the Competition for the provision of grants to teachers of MA course 2020/2021 of charity program „Vladimir Potanin Scholarship Program“. The work was supported by the Scientific and Educational School „Photonics and Quantum Technologies. Digital medicine“.

## Conflict of interest

The authors declare that they have no conflict of interest.

## References

- [1] D.S. Kopylova, N.Yu. Boldyrev, V.Ya. Yakovlev, Yu.G. Gladush, A.G. Nasibulin. *Kvantovaya elektronika*, **46** (12), 1163 (2016). DOI: 10.1070/QEL16146
- [2] S.J. Rezvani, D. Di Gioacchino, C. Gatti, C. Ligi, M.C. Guidi, S. Cibella, M. Fretto, N. Poccia, S. Lupi, A. Marcelli. *Condens. Matter*, **5** (2), 33 (2020). DOI: 10.3390/condmat5020033
- [3] A.S. Tukmakova, A.V. Asach, A.V. Novotelnova, I.L. Tkhorzhevskiy, N.S. Kablukova, P.S. Demchenko, A.D. Zaitsev, M.K. Khodzitsky. *Appl. Sci.*, **10** (6), 1929 (2020). DOI: 10.3390/app10061929
- [4] Z. Liu, Z. Liang, W. Tang, X. Xu. *Infrared Physics & Technology*, **105**, 103241 (2020). DOI: 10.1016/j.infrared.2020.103241
- [5] D.S. Ponomarev, D.V. Lavrukhin, A.E. Yachmenev, R.A. Khabibullin, I.E. Semenikhin, V.V. Vyurkov, M. Ryzhii, T. Otsuji, V. Ryzhii. *J. Phys. D.*, **51**, 135101 (2018). DOI: 10.1088/1361-6463/aab11d
- [6] P.M. Echternach, B.J. Pepper, T. Reck, C.M. Bradfort. *Nat. Astron.*, **2**, 90 (2018). DOI: 10.1038/s41550-017-0294-y
- [7] P. Seifert, X. Lu, P. Stepanov, J.R. Retamal, J.N. Moore, K.-C. Fong, A. Principi, D.K. Efetov. *Nano Lett.*, **20** (5), 3459 (2020). DOI: 10.1021/acs.nanolett.0c00373
- [8] P. Wang, H. Xia, Q. Li, F. Wang, L. Zhang, T. Li, P. Martyniuk, A. Rogalski, W. Hu. *Small*, **15**, 1904396 (2019). DOI: 10.1002/smll.201904396
- [9] A.V. Bogatskaya, N.V. Klenov, M.V. Tereshonok, A.M. Popov. *Tech. Phys. Lett.*, **44** (8), 667 (2018). DOI: 10.1134/S1063785018080059
- [10] A.E. Schegolev, A.M. Popov, A.V. Bogatskaya, P.M. Nikiforova, M.V. Tereshonok, N.V. Klenov. *JETP Lett.*, **111** (7), 371 (2020). DOI: 10.31857/S0370274X20070036
- [11] A.V. Bogatskaya, N.V. Klenov, P.M. Nikiforova, A.M. Popov, A.E. Schegolev. *Tech. Phys. Lett.*, **47** (9), 893 (2021). DOI: 10.1134/S1063785021090029
- [12] A.V. Bogatskaya, E.A. Volkova, N.V. Klenov, M.V. Tereshonok, A.M. Popov. *IEEE Trans. Antenn. Prop.*, **68** (6), 4831 (2020). DOI: 10.1109/TAP.2020.2972649
- [13] A.V. Bogatskaya, N.V. Klenov, M.V. Tereshonok, S.S. Adjemov, A.M. Popov. *J. Phys. D.*, **51** (18), 185602 (2018). DOI: 10.1088/1361-6463/aab756
- [14] A.W. Elshaari, I.E. Zadeh, A. Fognini, M.E. Reimer, D. Dalacu, Ph.J. Poole, V. Zwiller, K.D. Jöns. *Nature Comm.*, **8**, 379 (2017). DOI: 10.1038/s41467-017-00486-8
- [15] M.A. Remnev, V.V. Klimov. *Phys.-Usp.*, **61**, 157 (2018). DOI: 10.367/UFNe.2017.08.038192
- [16] L. Gu, Q. Yuan, Q. Zhao, Y. Ji, Z. Liu, L. Fang, X. Gan, J. Zhao. *Journal of Lightwave Technology*, **39**, 5069 (2021). DOI: 10.1109/JLT.2021.3082558w